Supplementary Information

Functional polysaccharide-coated SPIONs for in vitro mRNA delivery in breast cancer cells

Olga Tsave[1], Maria Psarrou[2,3], Georgia Kastrinaki[1,4], Eleni Papachristou[5], Rigini Papi[5], Vassilios Zaspalis[1,4], Lori Nalbandian[4†], Charalampos Sarafidis[6], Theodora Choli-Papadopoulou[5], Maria Vamvakaki[2,3], Christos Chatzidoukas[1,*]

[1] Department of Chemical Engineering, Aristotle University of Thessaloniki (AUTH), Thessaloniki, 54124, Greece

[2] Department of Materials Science and Technology, University of Crete, Vasilika Vouton, 70013, Heraklion, Crete, Greece

[3] Institute of Electronic Structure and Laser, Foundation of Research and Technology-Hellas, Vasilika Vouton, 70013, Heraklion, Crete, Greece

[4] Chemical Process & Energy Resources Institute (CPERI), Centre for Research & Technology Hellas (CERTH), Thessaloniki, Thermi, Greece

[5] Department of Chemistry, Aristotle University of Thessaloniki, GR-54124 Thessaloniki, Greece

[6] Department of Physics, Aristotle University of Thessaloniki, 54124 Thessaloniki, Greece

---

[*] *Corresponding author.* (Assist. Professor. C. Chatzidoukas)

Tel.: +30 2310 99 6167

E-mail address: chatzido@auth.gr

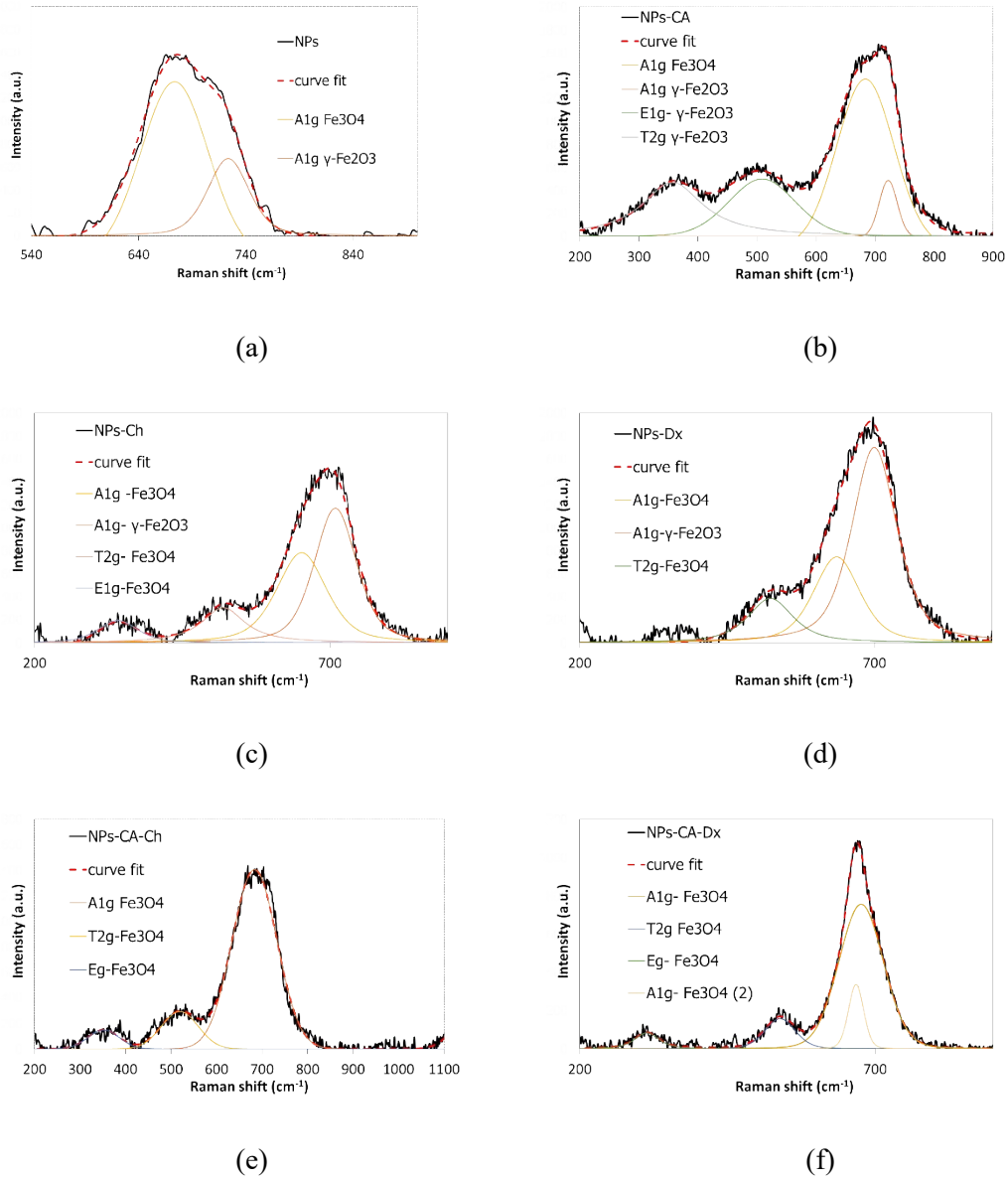

Fig. S1: Raman spectra and the deconvolution curves attributed to magnetite and maghemite for the (a) NPs, (b) NPs-CA, (c) NPs-Ch, (d) NPs-Dx, (e) NPs-CA-Ch and (f) NPs-CA-Dx samples.

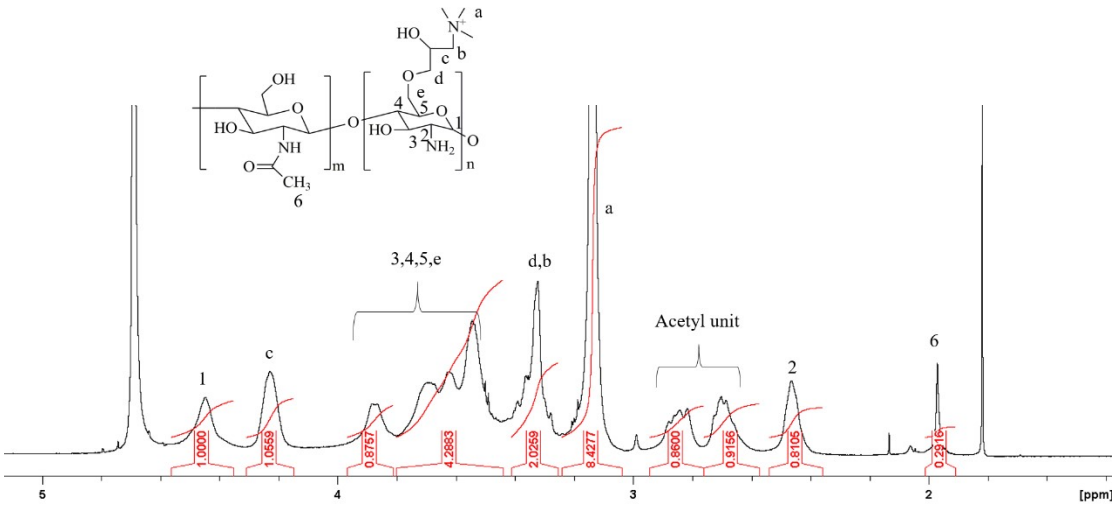

Fig. S2: ^{1}H NMR spectrum of Q-chitosan in D_2O.

The appearance of the characteristic chemical shift at 3.15 ppm in the ^{1}H NMR spectrum of Q-chitosan, assigned to the protons of the newly incorporated trimethyl ammonium groups (Fig. S2), verified the successful quaternization of the polymer.

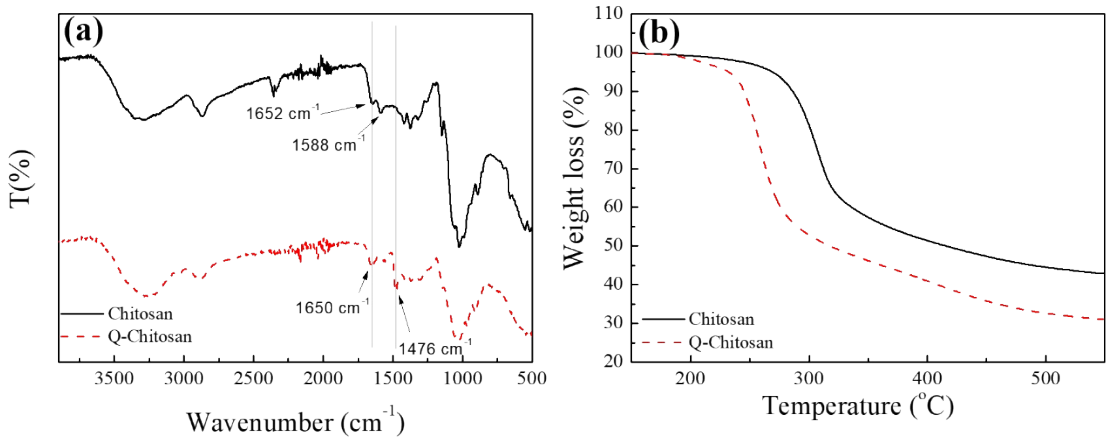

Fig. S3: (a) FTIR spectra and (b) TGA curves of chitosan (black solid line) and Q-chitosan (red dashed line).

The ATR-FTIR spectra of chitosan (black solid line) before quaternization, showed the vibration band at 1588 cm^{-1}, attributed to the amino groups and the shoulder at 1652 cm^{-1}, attributed to the amide bonds of the chitin units of chitosan [i]. After quaternization (Q-chitosan, red dashed line), a strong vibration band at 1476 cm^{-1}, which corresponds to the C-H bonds of the newly incorporated trimethyl ammonium groups, appeared, confirming the

successful quaternization of the biopolymer. Moreover, a peak at 1650 cm^{-1}, which corresponds to the primary amine groups of chitosan, which were not modified, was evident.

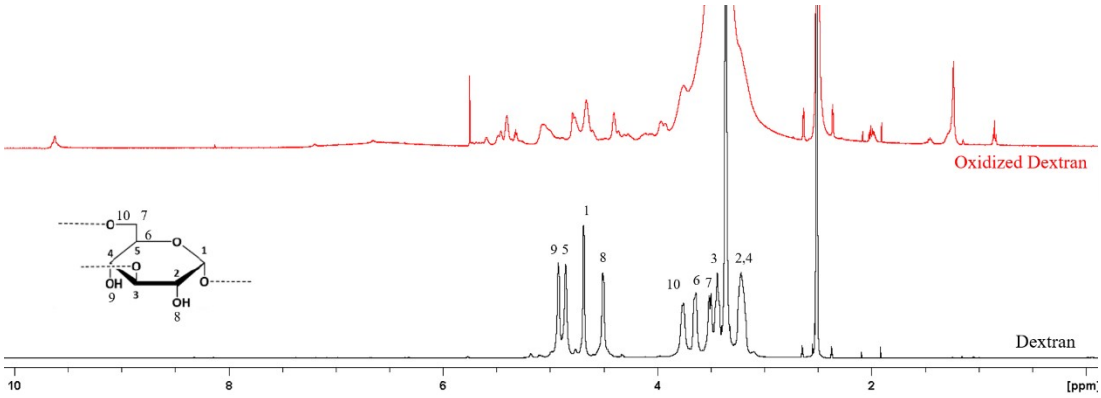

Fig. S4: ^{1}H NMR spectra of dextran and Ox-dextran in d_6-DMSO.

The appearance of a new peak at 9.3 ppm in the ^{1}H NMR spectrum of Ox-dextran denoted the successful modification of the polymer.

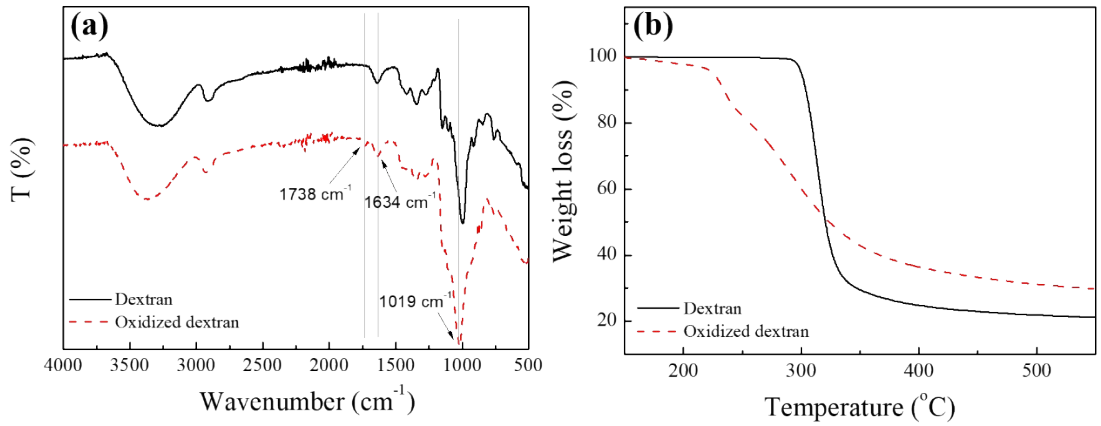

Fig. S5: (a) FTIR spectra and (b) TGA curves of dextran (black solid line) and Ox-dextran (red dashed line).

The ATR-FTIR spectrum of Ox-dextran showed the bands at 1019 and 1634 cm^{-1}, which were attributed to the vibrations of the C-O bonds and a characteristic vibration band of the carbonyl bond of the aldehyde group at 1738 cm^{-1}, verifying the successful oxidation of the polymer.

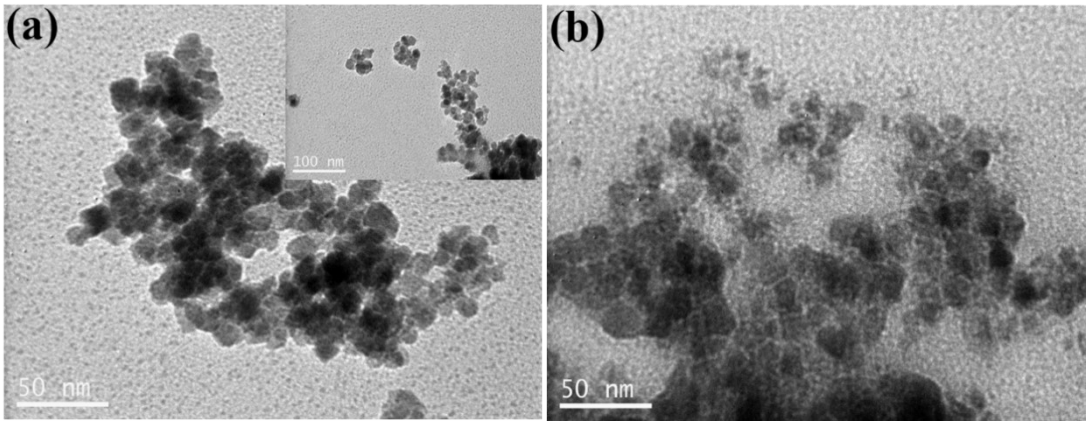

Fig. S6: TEM images of the (a) NPs-CA-Ch and (b) NPs-CA-Dx samples.

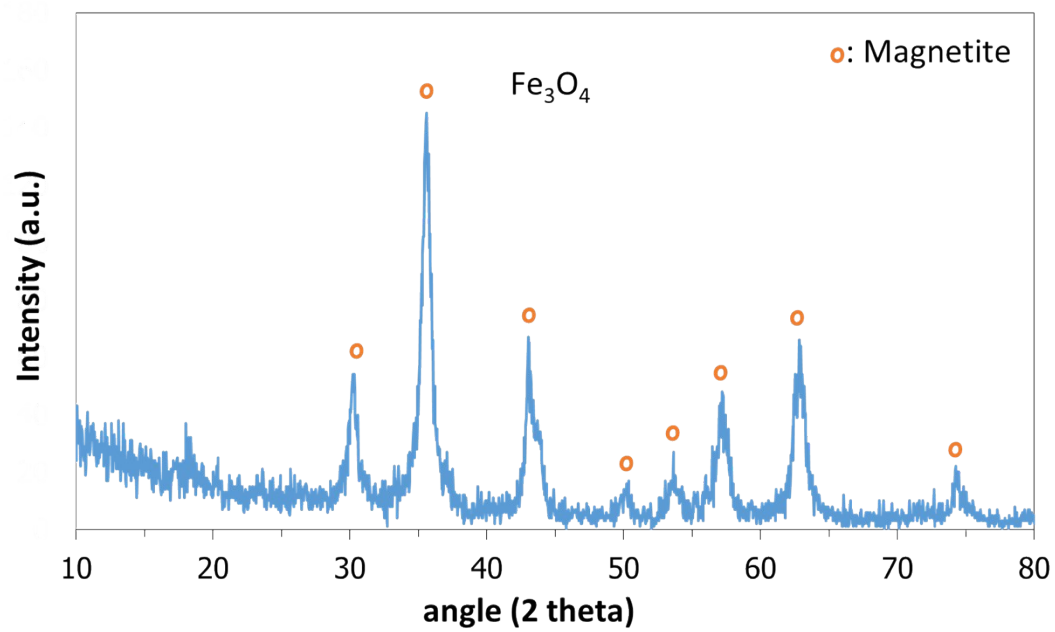

Fig. S7: XRD diagram of the bare Fe_3O_4 SPIONs.

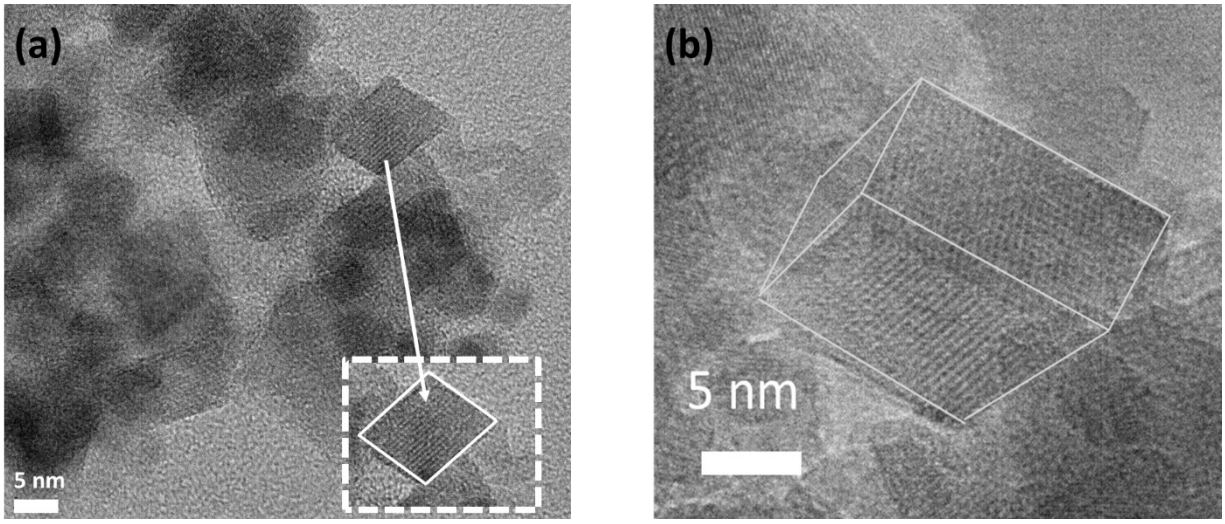

Fig. S8: (a) TEM image depicting agglomerates of NPs; the dashed line image shows a primary (single) particle defining with white outline the particle perimeter, (b) a high-resolution TEM image of a primary particle, defining with while outline the crystal planes of the cubic monocrystalline NP; the superparamagnetic NPs are monocrystalline

Fig. S8a illustrates the agglomerates of NPs as observed in TEM. In Fig. S8b, a primary cubic nanoparticle is depicted, revealing its monocrystalline nature through the orientation of planes in the three-dimensional structure. This observation aligns with the anticipated expectation, as SPIONs are known to be monocrystalline.

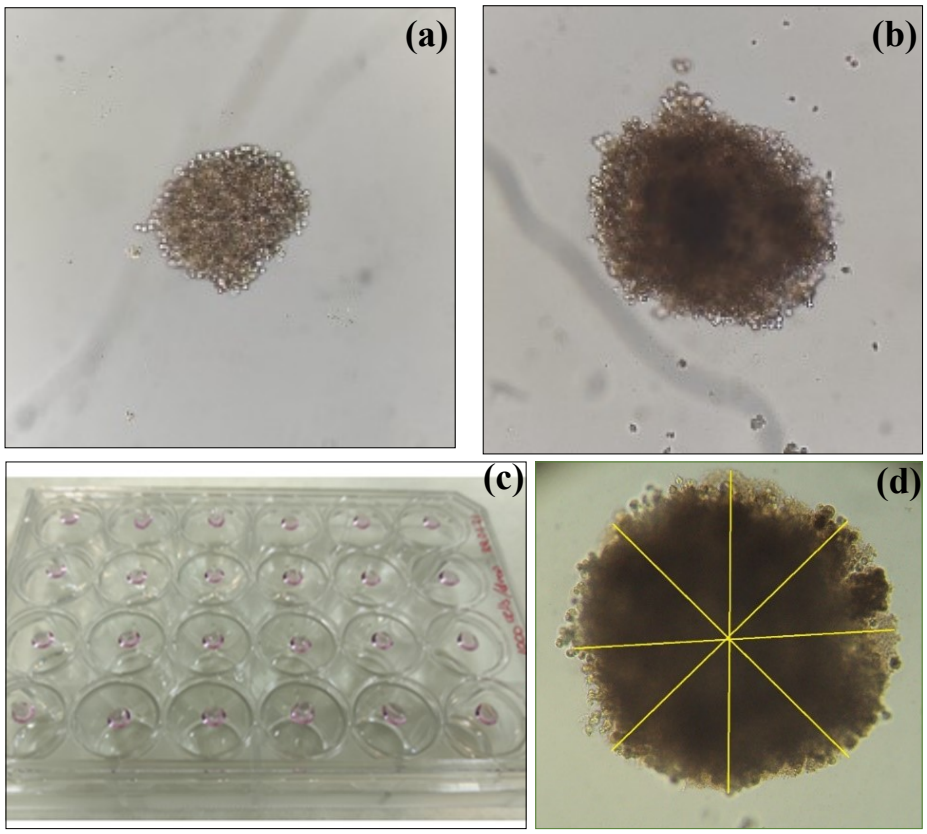

Fig. S9: (a), (b) Cell spheroid formation on days 3 and 12. (c) The hanging drop method. (d) Schematic representation of the diameter of each aggregate obtained as an average of 5 measurements.

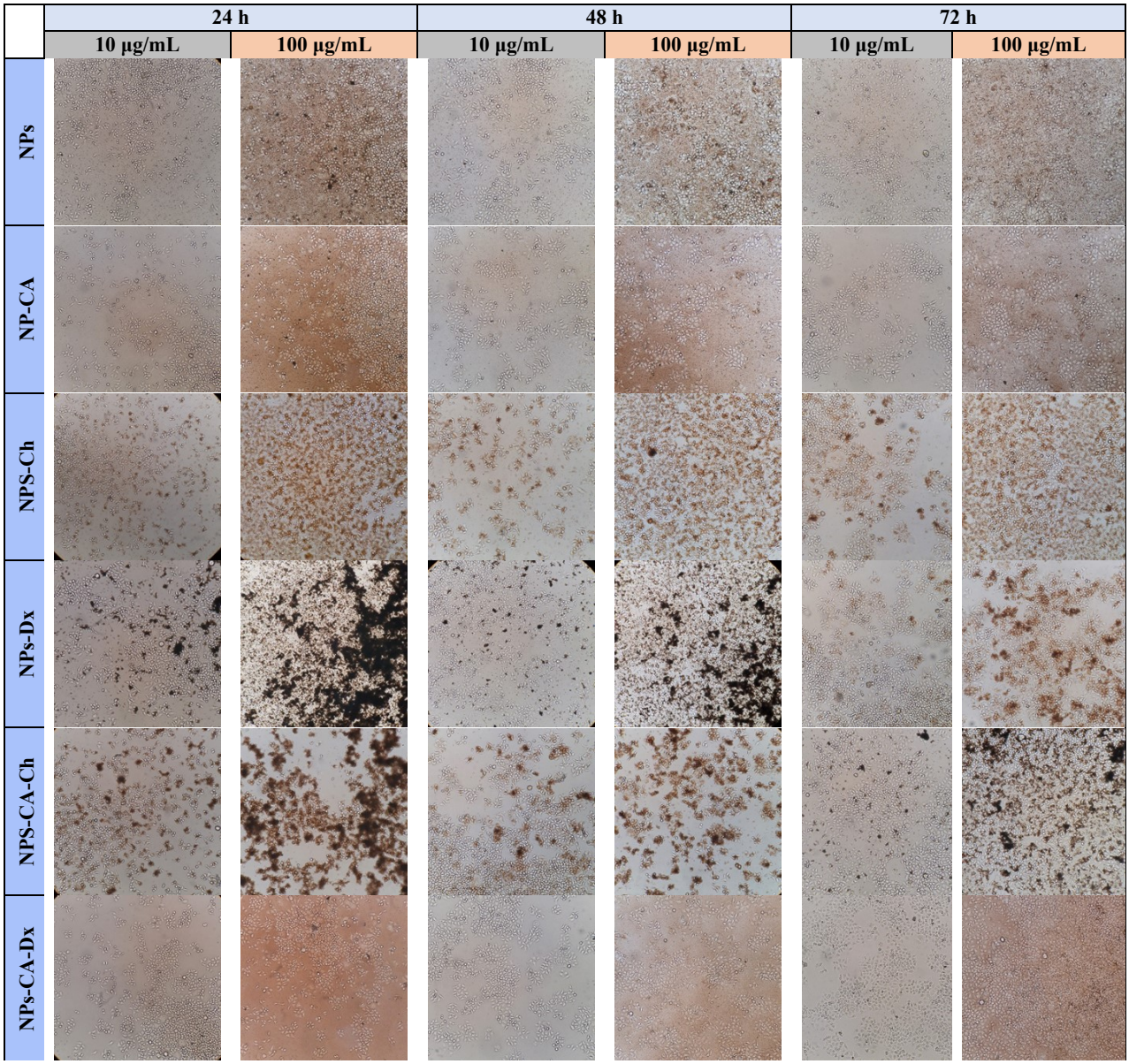

Fig. S10: Representative micrographs of cell adhesion of T47D cells following their treatment with SPIONs (photographs obtained using a LEICA inverted microscope, with a 10x phase contrast. Images were captured at several time points).

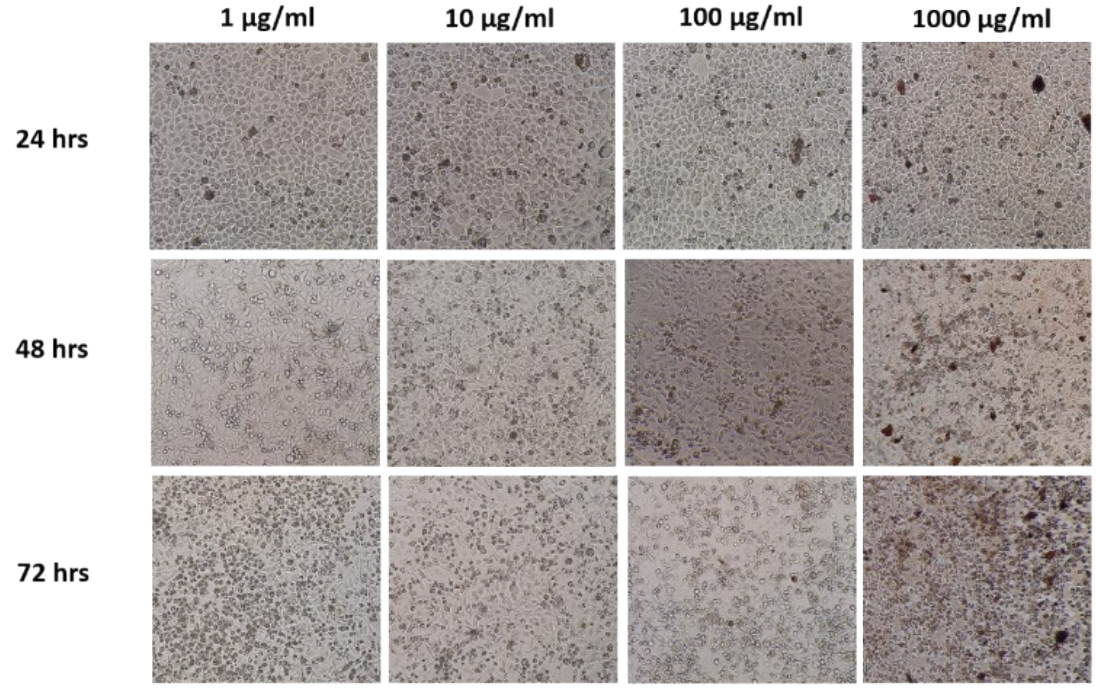
1 µg/ml
10 µg/ml
100 µg/ml
1000 µg/ml
24 hrs
48 hrs
72 hrs

NPs

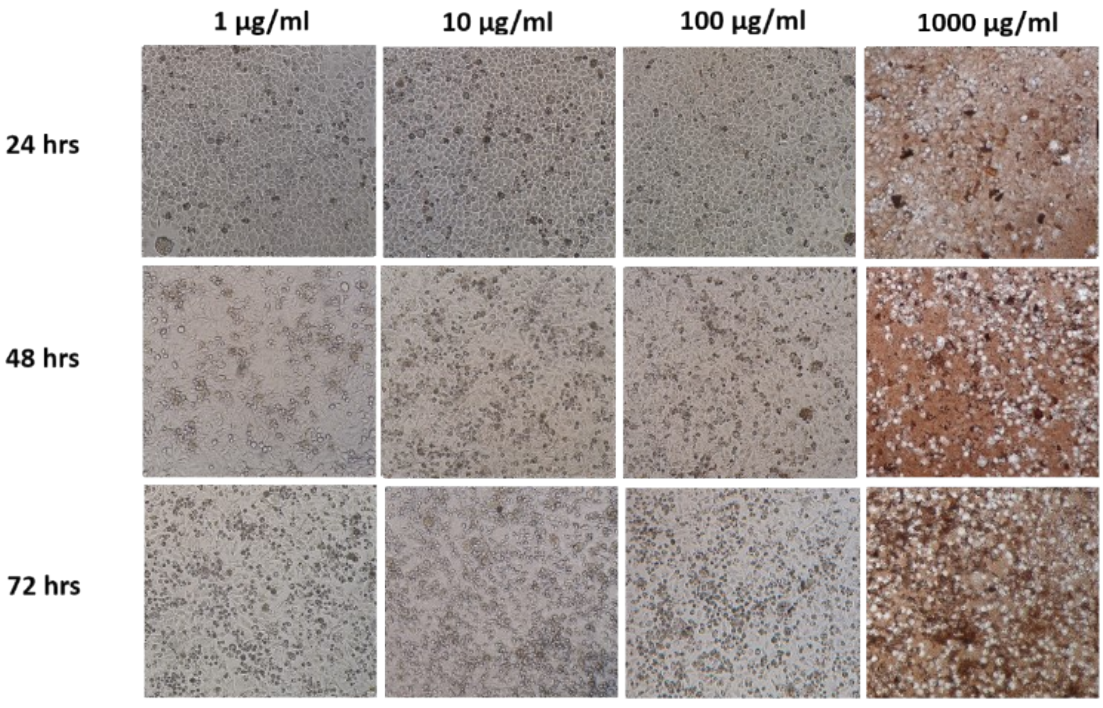
1 µg/ml
10 µg/ml
100 µg/ml
1000 µg/ml
24 hrs
48 hrs
72 hrs

NPs-CA

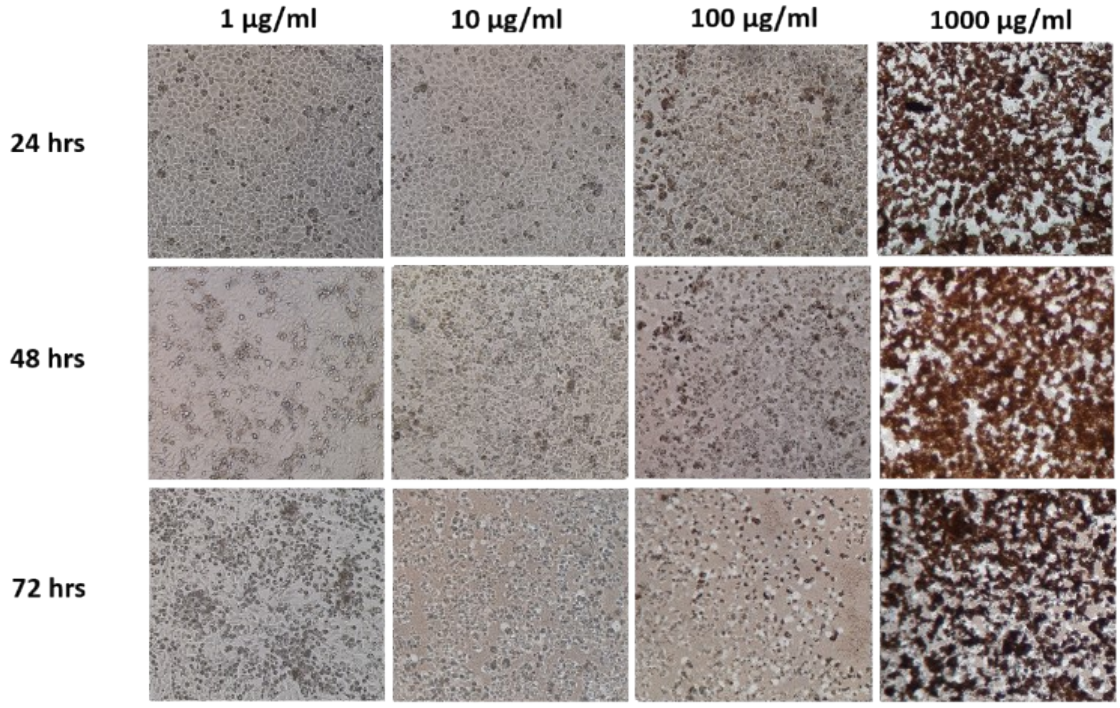

NPs-Ch

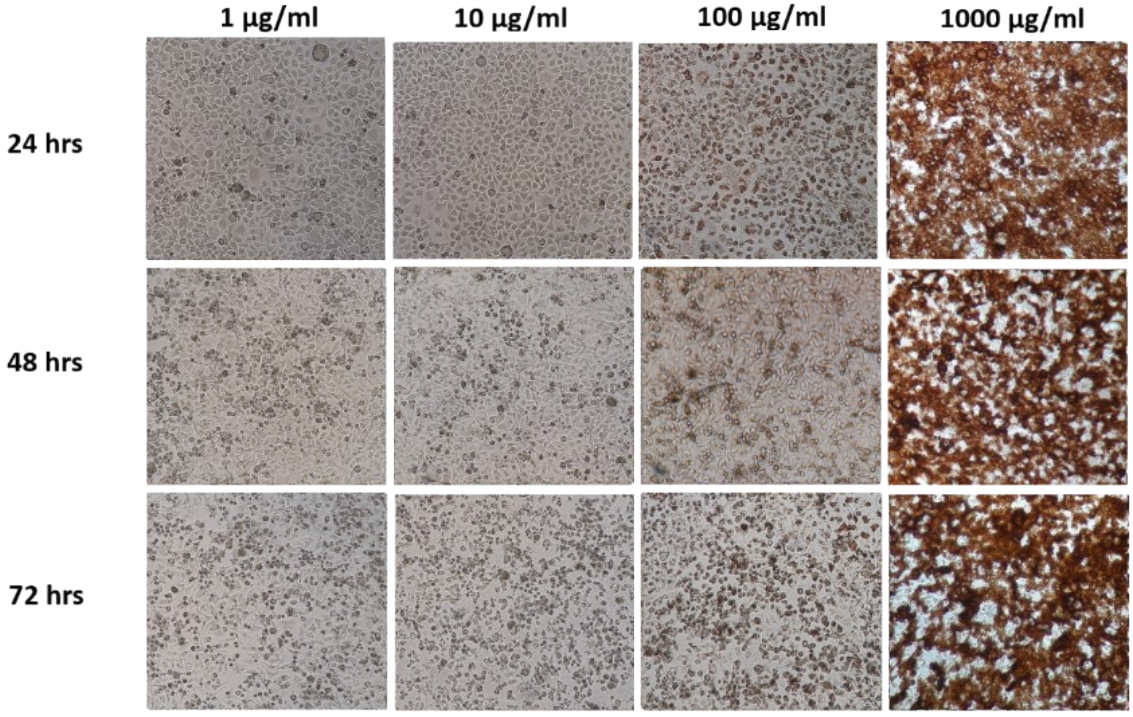

NPs-CA-Ch

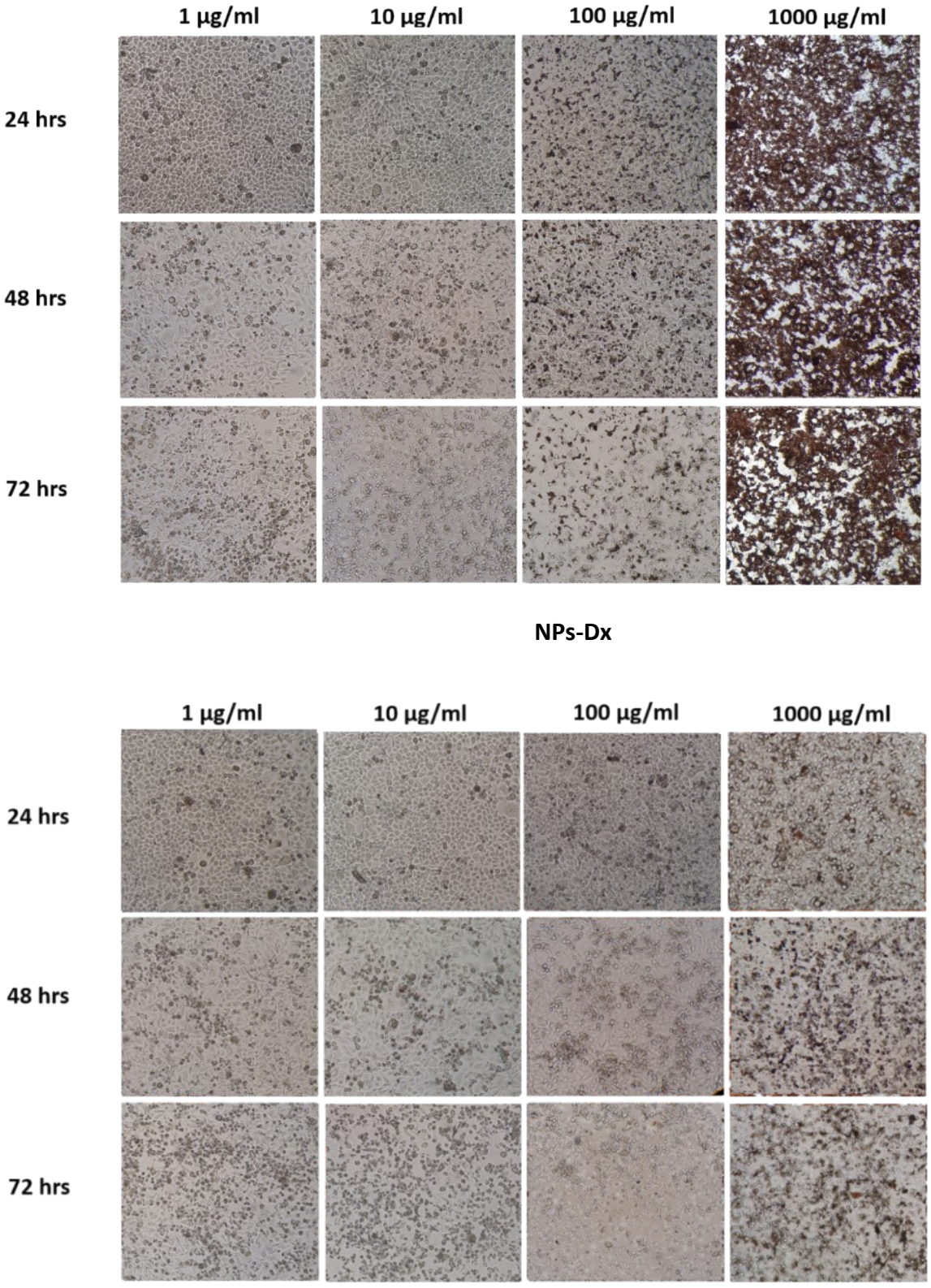

Fig. S11: Representative micrographs of cell morphology of T47D cells following their treatment with the SPIONs (photographs obtained using a LEICA inverted microscope, with a 10x phase contrast. Images were captured at several time points).

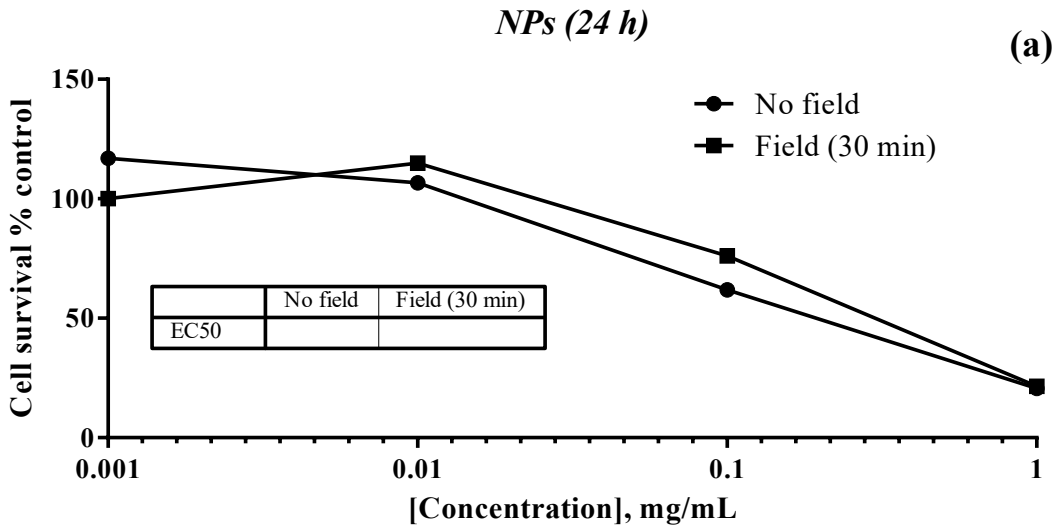
NPs (24 h)
(a)
Cell survival % control
150
100
50
0
0.001
0.01
0.1
1
[Concentration], mg/mL
No field
Field (30 min)
No field
Field (30 min)
EC50

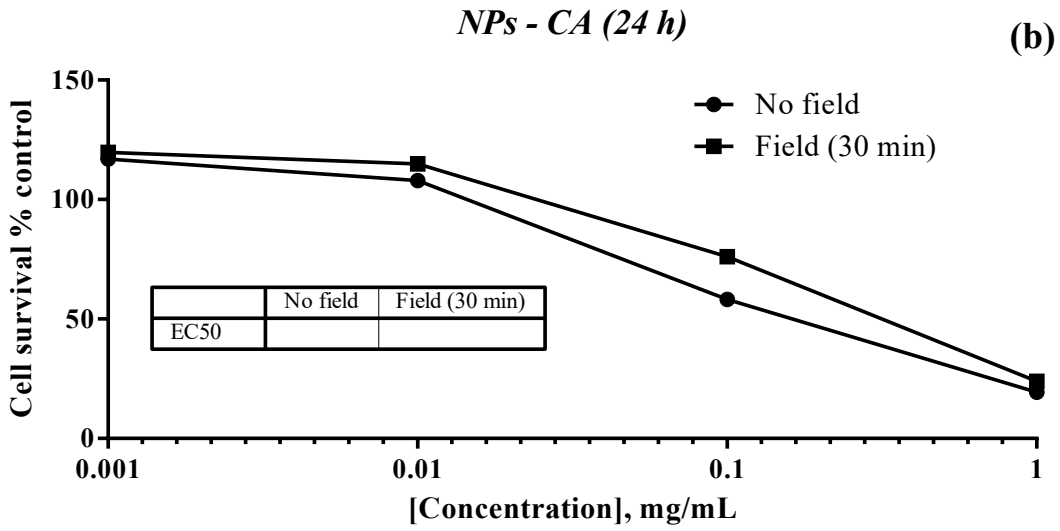
NPs - CA (24 h)
(b)
Cell survival % control
150
100
50
0
0.001
0.01
0.1
1
[Concentration], mg/mL
No field
Field (30 min)
No field
Field (30 min)
EC50

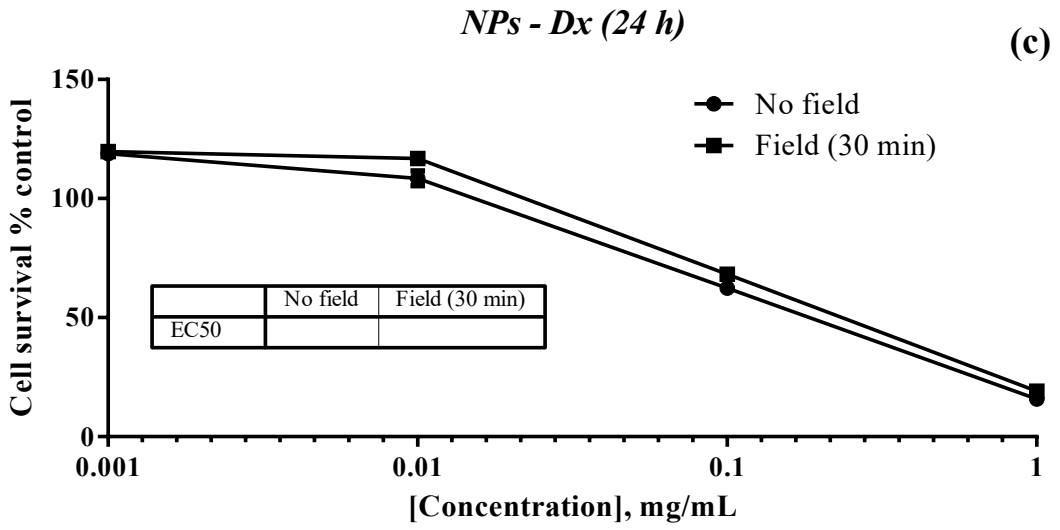
NPs - Dx (24 h)
(c)
Cell survival % control
150
100
50
0
0.001
0.01
0.1
1
[Concentration], mg/mL
No field
Field (30 min)
No field
Field (30 min)
EC50

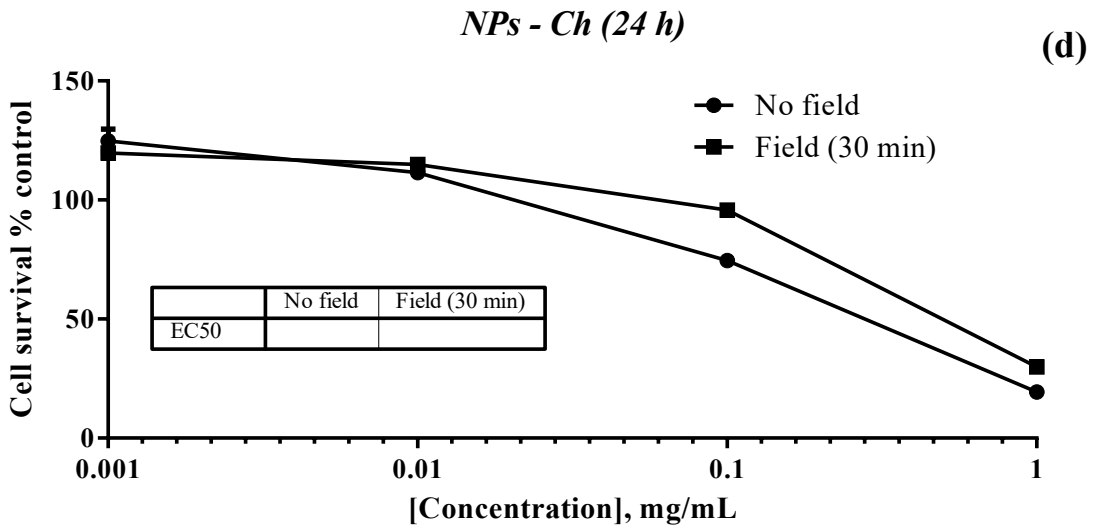

Fig. S12: Percentage change of cell survival of the T47D cells (2D monolayers), following treatment with various concentrations (1-1000 μM) of a) NPs, b) NPs-CA, c) NPs-Dx, and d) NPs-Ch for 24 h in the presence and absence of a magnetic field.

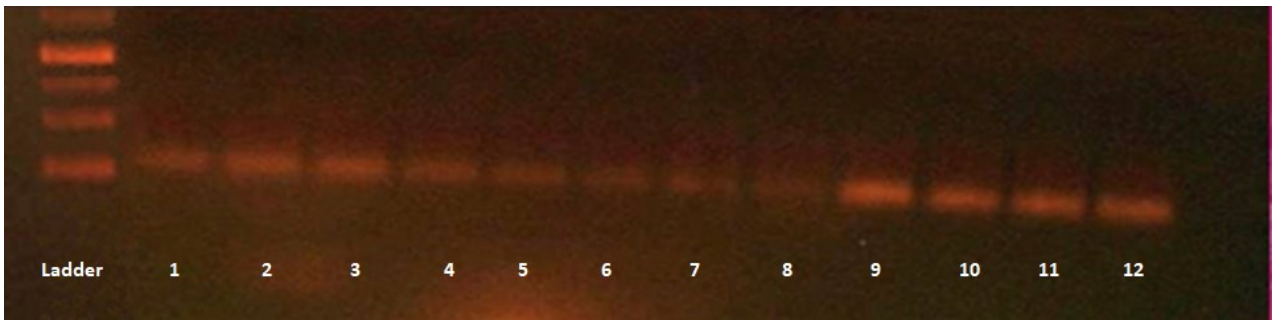

Fig. S13. Gel electrophoresis in 1% w/v agarose gel-to assess the efficient binding of GFP-mRNA onto the magnetic nanoparticles. Lane 1: NPs-Ch^{GFPmRNA} (ratio: 1/0.5); Lane 2: NPs-Dx^{GFPmRNA} (ratio: 1/0.5); Lane 3: NPs-Dx^{GFPmRNA} (ratio: 1/3); Lane 4: NPs-Ch^{GFPmRNA} (ratio: 1/3); Lane 5: NPs-CA-Ch^{GFPmRNA} (ratio: 1/0.5); Lane 6: NPs-CA-Ch^{GFPmRNA} (ratio: 1/1.5); Lane 7: NPs-CA-Ch^{GFPmRNA} (ratio: 1/3); Lane 8: NPs-CA-Ch^{GFPmRNA} (ratio: 1/5); Lane 9: NPs-CA-Dx^{GFPmRNA} (ratio: 1/0.5); Lane 10: NPs-CA-Dx^{GFPmRNA} (ratio: 1/1.5); Lane 11: NPs-CA-Dx^{GFPmRNA} (ratio: 1/3); Lane 12: NPs-CA-Dx^{GFPmRNA} (ratio: 1/5).

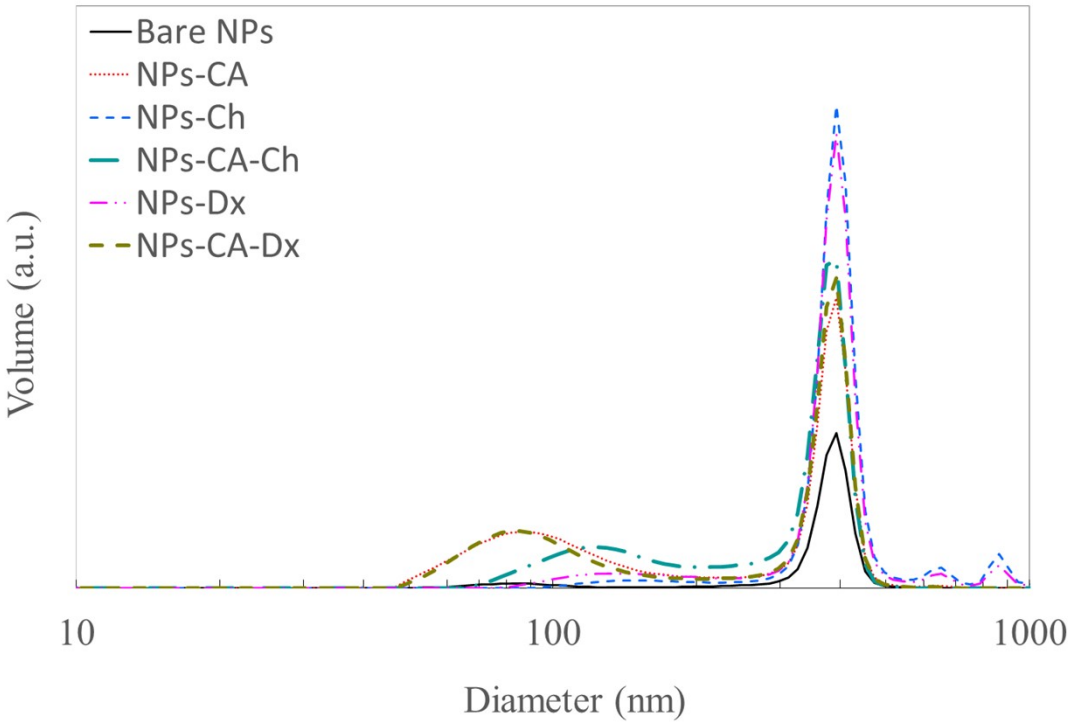

Figure S14: DLS Volume measurements of the bare NPs (black solid line), NPs-CA (red dotted line), NPs-Ch (blue short-dashed line), NPs-CA-Ch (green dashed-dotted line), NPs-Dx (magenta dashed dotted-dotted line) and NPs-CA-Dx (dark yellow dashed line).

i Wan, Y.; Creber, K.A.M.; Peppley, B.; Bui, V.T. Ionic conductivity of chitosan membranes. Polymer (Guildf). 2003, 44, 1057–1065, doi:10.1016/S0032-3861(02)00881-9.